

Supporting Information

Mechanochromic cyclemetalated cationic Ir(III) complex with AIE activity by strategic modifaciation of ligands

Yu Pei, Jiaxin Xie, Dongxu Cui, Shengnan Liu, Guangfu Li,* Dongxia Zhu,* and Zhongmin Su*

Key Laboratory of Nanobiosensing and Nanobioanalysis at Universities of Jilin Province, Department of Chemistry, Northeast Normal University, 5268 Renmin Street, Changchun, Jilin Province 130024, P.R. China. *E-mail: li00544@nenu.edu.cn, zhudx047@nenu.edu.cn, zmsu@nenu.edu.cn

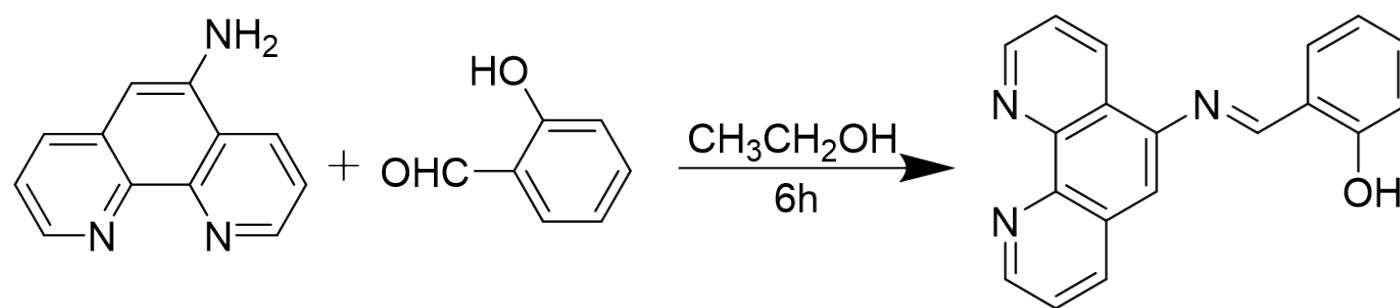
Table of Contents:	Page
1. Experimental - general information	S2
2. ¹ H NMR Spectrum of complex 1 at room temperature	S3
3. X-ray crystallographic data	S3
4. Photophysical data	S4

1. Experimental - general information

Materials obtained from commercial suppliers were used without further purification. All glassware, syringes, magnetic stirring bars, and needles were thoroughly dried in a convection oven. Reactions were monitored using thin layer chromatography (TLC). Commercial TLC plates were used and the spots were visualized under UV light at 254 and 365 nm. ^1H NMR spectra were performed on a Varian 500 MHz spectrometer with tetramethylsilane (TMS) as the internal standard. Elemental analyses were measured on a Flash EA1112 analyzer. The molecular weights of the two complexes were collected on matrix-assisted laser desorption-ionization time-of-flight (MALDI-TOF) mass spectrometry. The X-ray crystal data of the complexes were recorded by a Bruker Smart Apex II CCD diffractometer with graphite-monochromated Mo $K\alpha$ radiation ($\lambda = 0.71069 \text{ \AA}$). UV-vis absorption spectra were obtained by a Shimadzu UV-3100 spectrophotometer. The emission spectra were recorded by F-7000 FL spectrophotometer. The excited-state lifetime and photoluminescence quantum yields (PLQYs) were measured on using a transient spectrofluorimeter (Edinburgh FLS920). Transmission electron microscopy (TEM) and electron diffraction analyses were recorded by a TECNAI F20 microscope. Powder X-ray diffraction (PXRD) patterns of the different samples were obtained with a Rigaku Dmax 2000.

Synthesis of Schiff base ligand

5-amino-1,10-phenanthroline (528 mg, 2.71 mmol) and salicylaldehyde (412 mg, 2.38 mmol) were refluxed about 6h in 20 mL ethanol containing a catalytic amount of acetic acid. A suspension formed after refluxing. The mixture was then filtered hot, subsequently washed with hot ethanol affording the desired product as yellow solid. Yield: 874 mg (93 %).



Scheme S1 Synthetic route for Schiff base ligand.

2. ¹H NMR Spectrum of complex 1 at room temperature

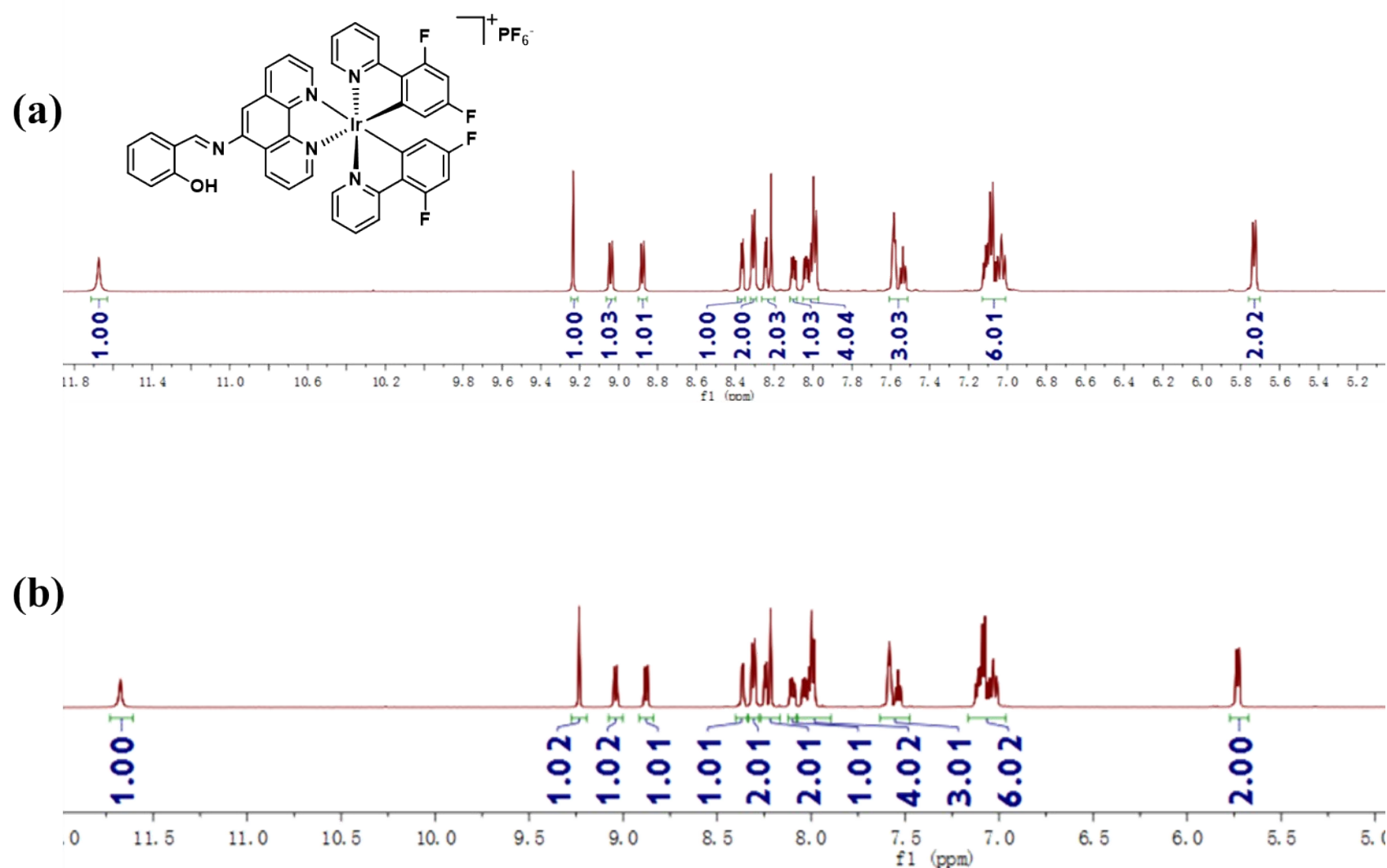


Fig. S1 ¹H NMR spectrum of complex 1 in DMSO-*d*₆ before grinding (a) and after grinding (b).

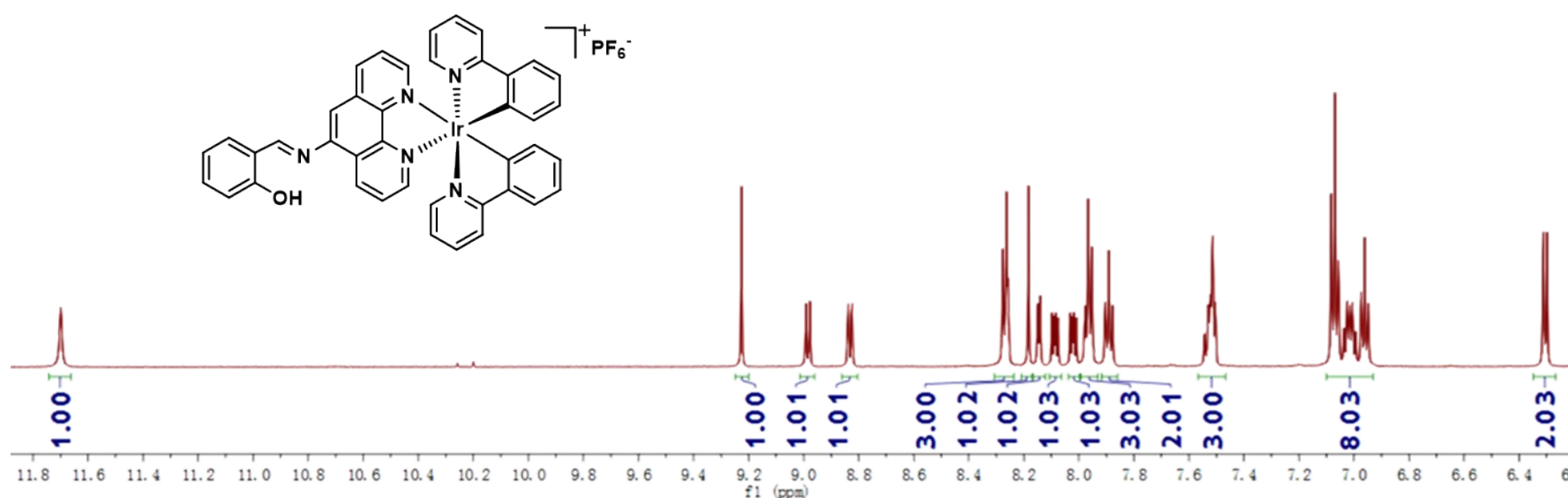


Fig. S2 ¹H NMR spectrum of complex 2 in DMSO-*d*₆.

3. X-ray crystallographic data

Diffraction data were collected on a Bruker SMART Apex CCD diffractometer using Cu K α ($\lambda = 1.54178$). Cell refinement and data reduction were made by the SAINT program. The structures were determined using the SHELXTL/PC program. Crystallographic data for them have been deposited with the Cambridge Crystallographic Data Centre with CCDC deposition number 2007989 and 2007993. These data can be obtained free of charge from The Cambridge Crystallographic Data Centre via www.ccdc.cam.ac.uk/data_request/cif.

Table S1 Crystal data and structure refinement for complexes **1** and **2**.

	1	2
Empirical formula	C ₄₁ H ₂₅ F ₁₀ IrN ₅ OP	C ₄₁ H ₂₉ F ₆ IrN ₅ OP
Formula weight	1016.85	944.88
Temperature (K)	173	173
Crystal system	triclinic	monoclinic
space group	P $\bar{1}$	C2/c
a /Å	10.5032(3)	21.9461(13)
b /Å	11.9399(4)	13.7526(7)
c /Å	18.1307(6)	27.5646(14)
α /°	88.758(1)	90
β /°	76.633(1)	91.034(2)
γ /°	74.371(1)	90
V/Å ³	2128.33(12)	8318.1(8)
Z	2	8
ρ_{calc} (g/cm ³)	1.587	1.509
μ /mm ⁻¹	7.154	3.312
R _{int}	0.0506	0.0338
Goodness-of-fit on F ²	1.057	1.130
R ₁ ^a , wR ₂ ^b [I>2 σ (I)]	0.0286,0.0733	0.0252,0.0605
R ₁ , wR ₂ (all data)	0.0303,0.0742	0.0301,0.0620

^a $R_1 = \sum ||F_o| - |F_c|| / \sum |F_o|$. ^b $wR_2 = \{ \sum [w(F_{o2} - F_c)^2] / \sum [w(F_o^2)^2] \}^{1/2}$

4. Photophysical data

Table S2 Photophysical characteristics of complexes **1** and **2**.

Absorption and emission at room temperature					$k_r \times 10^6 \text{ s}^{-1}$	$k_{nr} \times 10^6 \text{ s}^{-1}$	
	λ_{abs}^a (nm)	λ_{em}^a (nm)	λ_{em}^b (nm)	Φ_{em}^b	τ^b (μs)		
1	363(0.963)	571	549	0.06	2.58	0.023	0.36
2	385(1.048)	591	598	0.02	5.46	0.004	0.18

^a Measured in CH₃CN (1.0 \times 10⁻⁵ M) solution. ^b Measured in solid state .

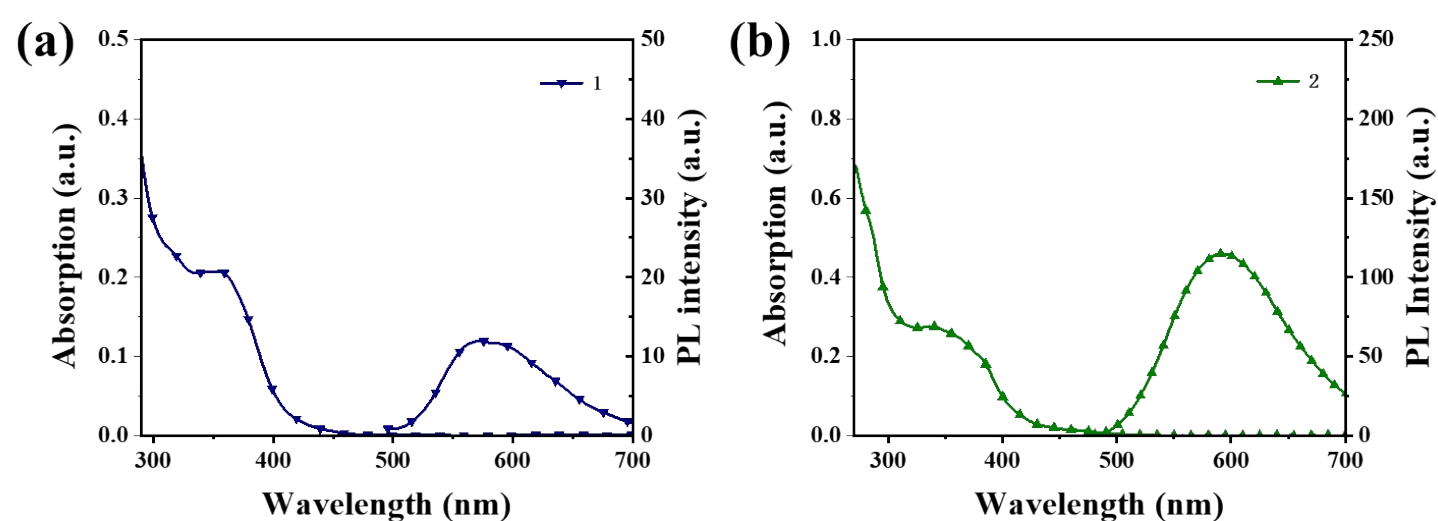


Fig. S3 Absorption and emission spectra of complexes **1** (a) and **2** (b) in CH_3CN solution (1.0×10^{-5} M) at room temperature.

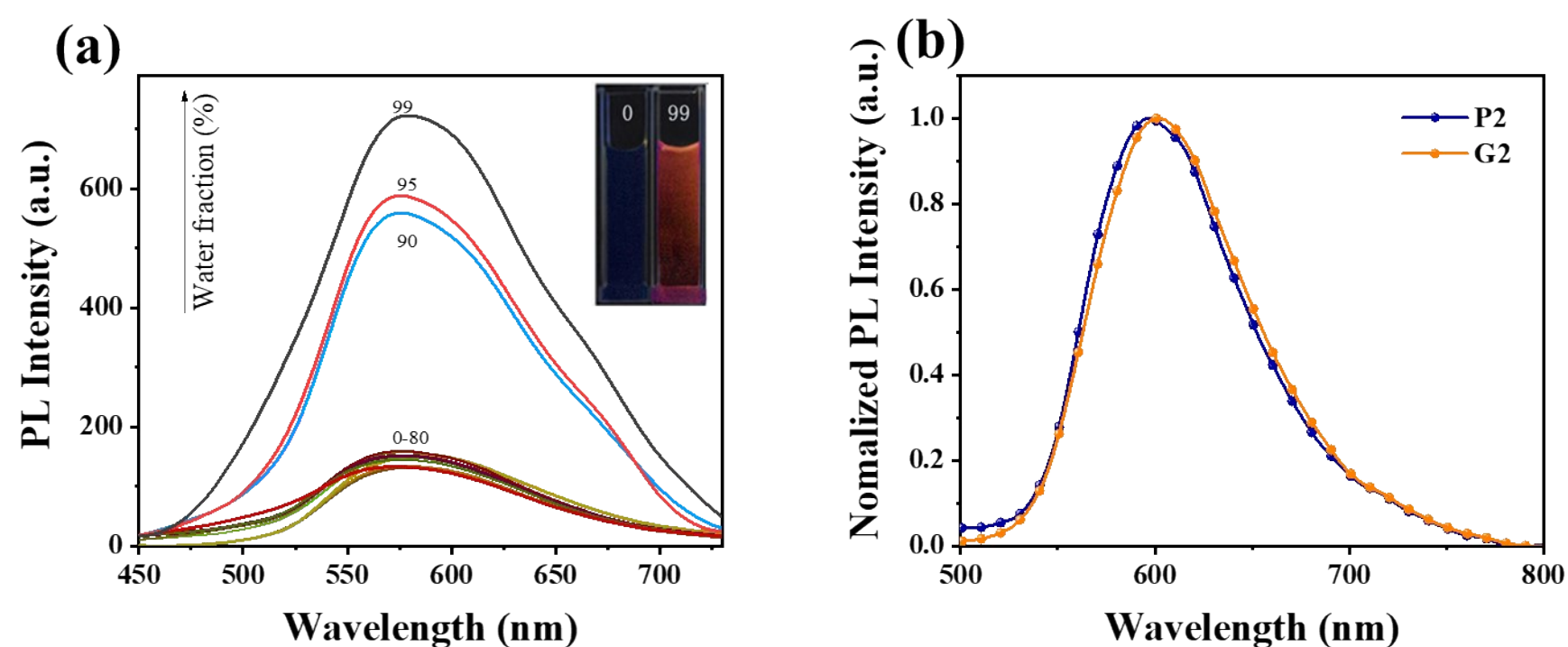


Fig. S4 (a) The emission spectra of complex **2** in water- CH_3CN mixtures with different water fractions (0–99% v/v) at room temperature. Inset: Emission image of complex **2** in pure CH_3CN solution and a water- CH_3CN mixture (99% water fraction) under 365 nm UV illumination. (b) Normalized emission spectra of the sample **2** as indicated.

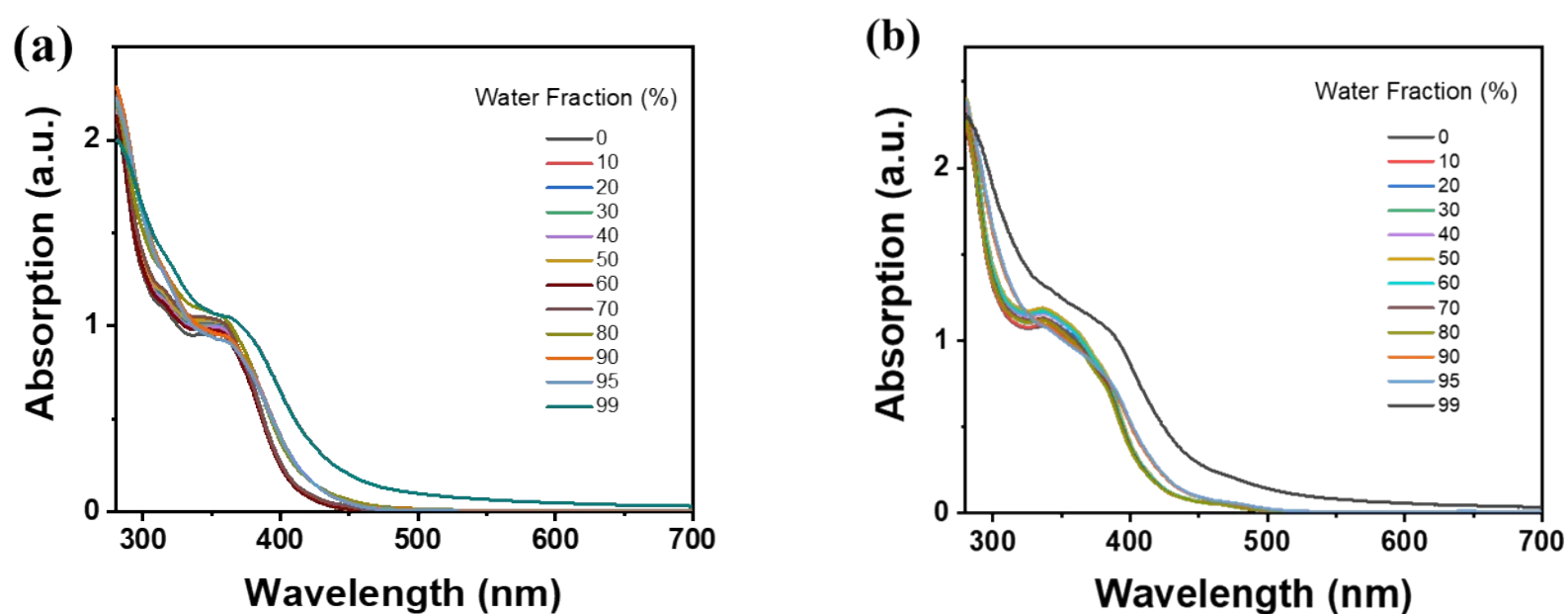


Fig. S5 Absorption spectra of complex **1** (a) and complex **2** (b) in CH_3CN - H_2O mixtures (complex concentration = 1.0×10^{-5} M) with different water fractions (0–99%, v/v) at room temperature.

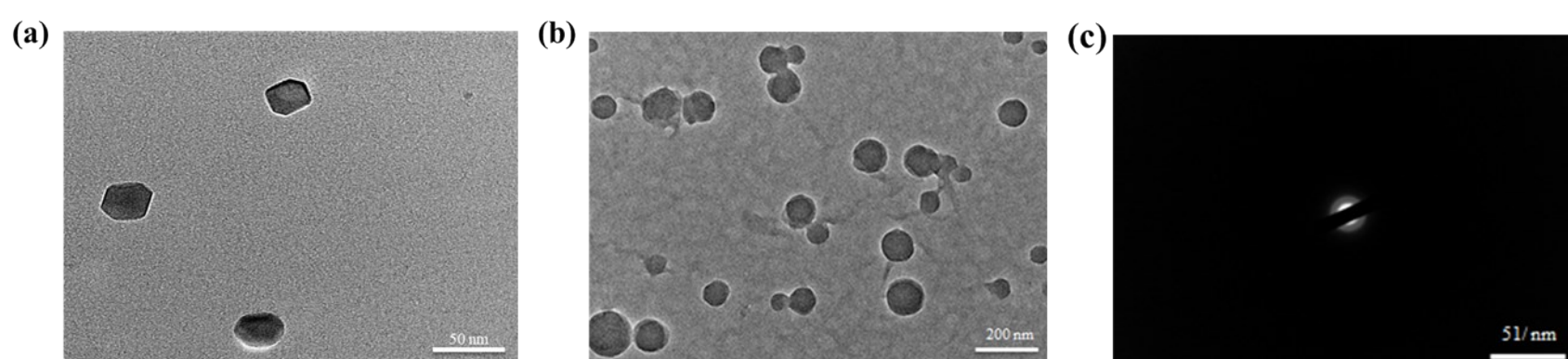


Fig. S6 TEM image of nanoaggregates of complex **1** formed in water-CH₃CN mixtures with 0% (a) and 99% (b) water fraction. (c) Electron diffraction pattern of the amorphous nanoaggregates.

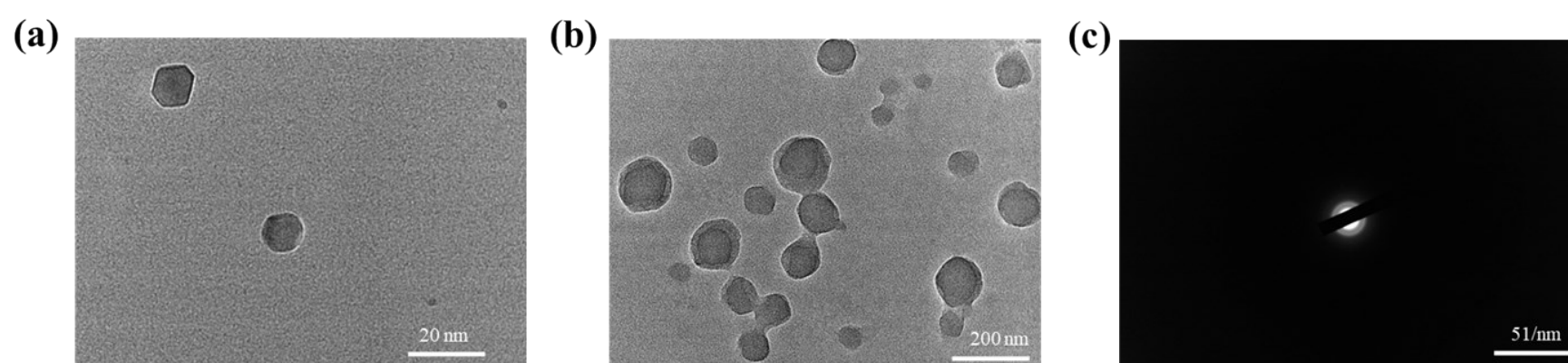


Fig. S7 TEM image of nanoaggregates of complex **2** formed in water-CH₃CN mixtures with 0% (a) and 99% (b) water fraction. (c) Electron diffraction pattern of the amorphous nanoaggregates.

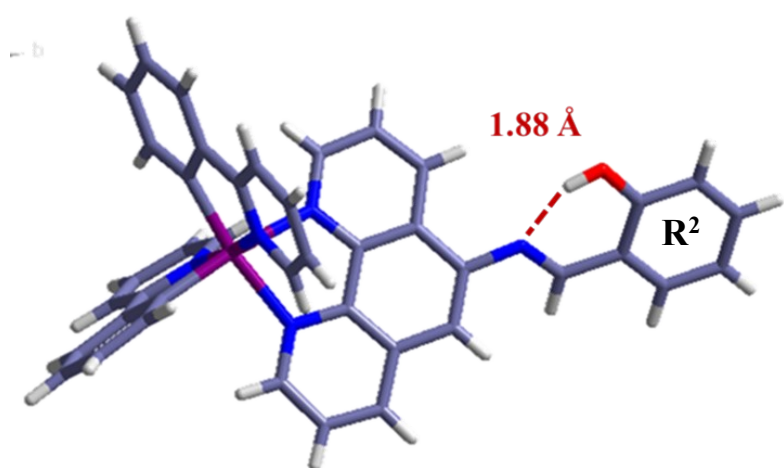


Fig. S8 Intramolecular O-H...N hydrogen bond of complex **2**.

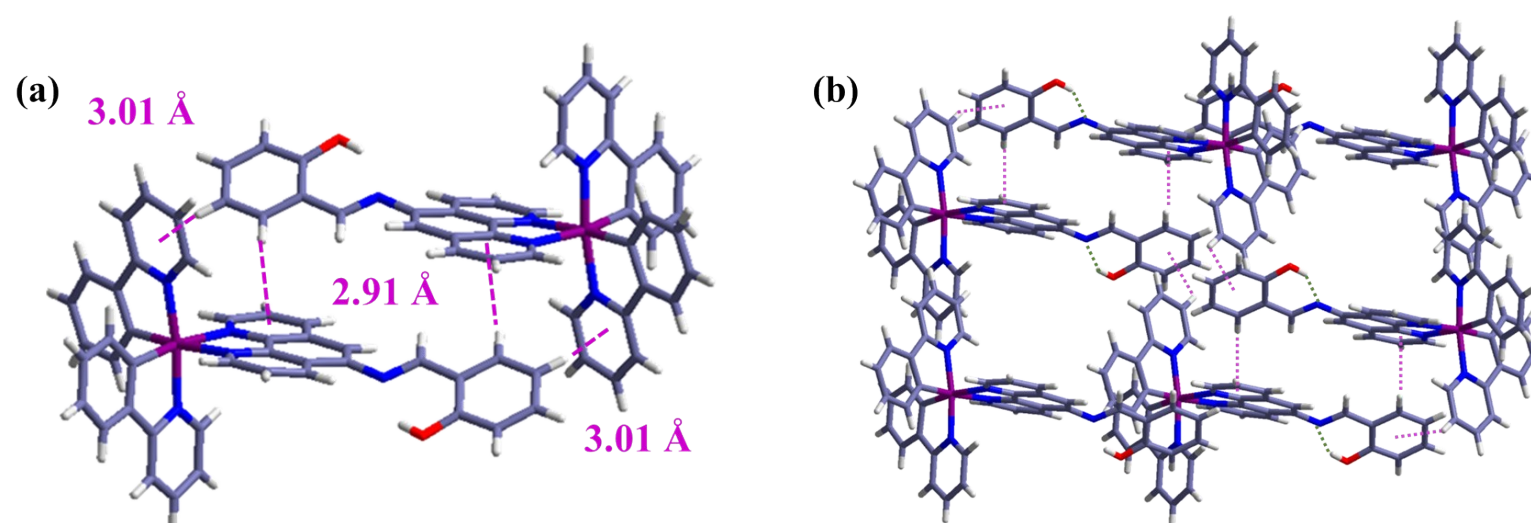


Fig. S9 (a) Intermolecular C-H...π interactions; (b) schematic supramolecular structure of complex **2**.